

Parametric Oscillation, Frequency Mixing, and Injection Locking of Strongly Coupled Nanomechanical Resonator Modes

Maximilian J. Seitner,^{1,*} Mehdi Abdi,^{2,3} Alessandro Ridolfo,⁴ Michael J. Hartmann,⁵ and Eva M. Weig¹

¹*Department of Physics, University of Konstanz, 78457 Konstanz, Germany*

²*Department of Physics, Technische Universität München, 85748 Garching, Germany*

³*Institute for Theoretical Physics, Ulm University, 89081 Ulm, Germany*

⁴*Dipartimento di Scienze Matematiche e Informatiche, Scienze Fisiche e Scienze della Terra (MIFT), Università di Messina, 98166 Messina, Italy*

⁵*Institute of Photonics and Quantum Sciences, Heriot-Watt University, EH14 4AS Edinburgh, United Kingdom*

(Received 6 December 2016; published 20 June 2017)

We study locking phenomena of two strongly coupled, high quality factor nanomechanical resonator modes to a common parametric drive at a single drive frequency in different parametric driving regimes. By controlled dielectric gradient forces we tune the resonance frequencies of the flexural in-plane and out-of-plane oscillation of the high stress silicon nitride string through their mutual avoided crossing. For the case of the strong common parametric drive signal-idler generation via nondegenerate parametric two-mode oscillation is observed. Broadband frequency tuning of the very narrow linewidth signal and idler resonances is demonstrated. When the resonance frequencies of the signal and idler get closer to each other, partial injection locking, injection pulling, and complete injection locking to half of the drive frequency occurs depending on the pump strength. Furthermore, satellite resonances, symmetrically offset from the signal and idler by their beat note, are observed, which can be attributed to degenerate four-wave mixing in the highly nonlinear mechanical oscillations.

DOI: [10.1103/PhysRevLett.118.254301](https://doi.org/10.1103/PhysRevLett.118.254301)

The development of lasers and masers opened up the path to the realm of controlled nonlinear physics. If a material with a nonlinear susceptibility is strongly pumped above a certain threshold by a coherent drive source, its response exhibits characteristic nonlinear effects. The Kerr effect, second-harmonic generation, spontaneous parametric down-conversion, or four-wave mixing are just some prominent examples for the great variety of nonlinear physical effects [1]. Installing the nonlinear medium inside a resonant cavity leads to the concept of parametric oscillators, in particular the optical parametric oscillator (OPO) [2]. During the past decades, this model system has been exploited to study a variety of parametric effects including injection locking [3], where an oscillator is strongly pumped at a frequency close to its natural resonance frequency. If the amplitude of the pump exceeds a threshold value, the oscillator will lock to the pump in frequency and/or phase. This phenomenon was originally proposed by Adler [4] and has been studied in a variety of systems, for example, semiconductor lasers [5–8], electrical oscillators [9–12], organ pipes [13,14], and micro-masers [15] amongst others.

For the case of simultaneous frequency and phase locking in combination with the reduction of phase noise, synchronization of two or more oscillators to a reference oscillator or to each other [4] is observed.

Recently, the study of parametric oscillation [16–19], thermal-noise two-mode squeezing [20–23], and synchronization phenomena has been transferred to mechanical

microresonators [24–30] and the field of cavity opto- or electromechanics. In the latter case, special attention needs to be paid to distinguish between the demonstration of real synchronization as originally defined above [31–36] and the mixing and locking phenomena of oscillators [37–43].

In this work, we demonstrate a set of characteristic nonlinear physical effects in a nanoelectromechanical system by investigating different parametric driving regimes of strongly coupled, high quality factor nanomechanical resonator modes subject to a joint strong parametric pump. In particular, we observe frequency mixing products that are analogous to second-order and third-order nonlinear effects in nonlinear optical systems. Depending on the frequency difference of the two modes and the strength of the parametric drive, we observe broadband frequency tunable signal-idler generation via nondegenerate parametric two-mode oscillation (NDP2O), satellite resonances induced by degenerate four-wave mixing (D4WM), partial injection locking including injection pulling, and injection locking over a large frequency range. The effects are investigated by measuring the frequency spectra of the two coupled nanomechanical resonator modes near the avoided energy level crossing.

The employed nanoelectromechanical system (cf. the Supplemental Material [44]) consists of the flexural in-plane (in) and out-of-plane (out) mode of a 55 μm long, 270 nm wide, and 100 nm thick doubly clamped silicon nitride string resonator operated in vacuum at room temperature, which is flanked by two adjacent gold electrodes. A dc voltage applied

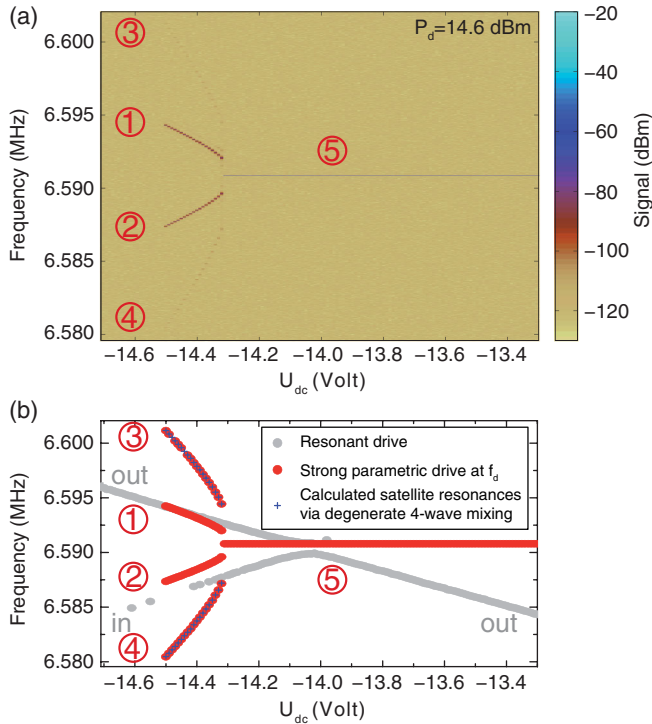


FIG. 1. (a) Color-coded frequency spectra versus dc voltage for a strong parametric drive power $P_d = 14.6$ dBm at $f_d = 13.18163$ MHz. Parametric oscillation resonances (f_1, f_2), satellites from degenerate four-wave mixing (f_3, f_4), and complete injection locking (f_5) to half of the drive frequency are observed. (b) The extracted peak frequencies of the above spectra (red dots) and calculated satellite resonances from Eq. (2) (blue daggers) exhibit excellent agreement. The gray dots display the avoided crossing of the two modes under a weak resonant drive with a mode splitting of 0.97 kHz. Some gray dots are missing for the in-plane mode due to the bad detection efficiency of this mode.

to the electrodes enables dielectric tuning ($\propto U_{dc}^2$) of the resonance frequencies ($f_{out} \approx f_{in} \approx 6.5$ MHz) via electric gradient fields [45]. When the two modes are tuned into resonance they hybridize into normal modes, i.e., linear combinations of in-plane and out-of-plane modes, and exhibit a pronounced avoided crossing. This reflects the strong coupling of the nanomechanical two-mode system [46–48]. The mechanical modes exhibit a high mechanical quality factor near 500 000, which reduces quadratically with the applied dc voltage [45]. A microwave cavity connected via the same two electrodes is employed for signal transduction and heterodyne read-out [49].

We investigate the dynamics of the two coupled modes in the vicinity of the avoided crossing under a strong common parametric drive tone for drive powers between $P_d = -1.5$ dBm and $P_d = 15$ dBm by applying the following measurement scheme.

We initialize the system to the left-hand side of the avoided crossing by choosing an appropriate dc voltage (see e.g. Fig. 1). At this point, the two modes are thermally excited at their resonance frequencies by the thermal noise

of the room temperature environment. Note that the thermal amplitudes of the two modes are too small to be resolved in the frequency spectra discussed in the following. A nonresonant strong sinusoidal drive tone at f_d is continuously applied to the system. This parametric drive tone, modulating the resonant frequencies at approximately twice the eigenfrequencies of the out-of-plane and in-plane mode, $f_d \approx 2f_{out} \approx 2f_{in}$, is also applied to the electrodes as a corresponding rf voltage $U_d \propto \sqrt{P_d} \sin(2\pi f_d t)$. Note that this rf voltage does not effectuate a resonant driving for the lack of a mechanical mode at this frequency and hence the system can be viewed as a pair of nondegenerate parametric oscillators [20,23,50]. By changing the dc voltage, the two thermally excited resonances are tuned through the avoided crossing where we record the mechanical frequency spectra for each particular U_{dc} .

Prior to each measurement, the avoided crossing of the two modes is recorded in the weakly driven regime by tuning the dc voltage, where the mechanical modes are resonantly excited by a weak 10 MHz bandwidth noise drive. The coupling strength is determined from the avoided crossing data. A center frequency f_c is chosen as a frequency in between the two modes at the avoided crossing frequency splitting. Note that f_c does not need to be chosen as the mean of the two respective mode frequencies. The frequency of the strong parametric sinusoidal drive tone f_d corresponds to twice the center frequency $f_d = 2f_c$.

Figure 1(a) depicts the color-coded frequency spectra for a strong parametric drive of $P_d = 14.6$ dBm. In Fig. 1(b) the extracted parametric oscillation peaks of the frequency spectra are displayed as red dots. The gray dots visualize the response of the system under a weak resonant driving, i.e., the avoided crossing of in-plane (f_{in}) and out-of-plane (f_{out}) resonances with a level splitting of 0.97 kHz. At a voltage of $U_{dc} = -14.5$ V two sharp frequency peaks at $f_1 \approx f_{out}(-14.5$ V) and $f_2 \neq f_{in}(-14.5$ V) suddenly appear. From the extracted frequencies we find

$$f_1 + f_2 = f_d = 2f_c, \quad (1)$$

which mimics the signal-idler generation process in optical parametric oscillation [2]. The strong pump at f_d parametrically amplifies the thermally excited resonances of the out-of-plane mode (signal) and the in-plane mode (idler) if their resonance frequencies get close enough to half of the pump frequency (NDP2O above the parametric instability threshold). The NDP2O appears due to the coupling of the two modes, where we denote the out-of-plane parametric oscillation (f_1) as the signal, and the in-plane parametric oscillation ($f_2 = f_d - f_1$) as the idler, since $f_1 \approx f_{out}$. The fact that the idler frequency f_2 differs from the resonance frequency of the natural in-plane mode clearly establishes the analogy to the process of signal-idler generation via the OPO in a doubly resonant cavity, which is a second-order nonlinear optical effect. The in-plane mode is forced to oscillate at a frequency f_2 determined from the frequency-matching

condition (1), which is analogous to the phase-matching condition in the OPO [2]. In the present experiment, the optical cavity is replaced by the two flexural modes of the nanomechanical string resonator and the nonlinear optical medium corresponds to the highly nonlinear response of the resonant modes under parametric oscillation. The mechanical nonlinearity is intrinsic to the material and becomes apparent because of the high mechanical quality factors and the corresponding large vibration amplitudes of the in-plane and out-of-plane mode. After the parametric instability threshold, we are able to tune the two sharp parametric resonances towards each other in frequency as a function of the dc voltage. In this way, we are able to independently tune the NDP2O by approximately 2.5 kHz, which corresponds to roughly 100 times the linewidth of the natural in-plane and out-of-plane resonances, hence establishing a broadband-tunable, very narrow linewidth two-mode parametric oscillator. Note that the tuning behavior slightly deviates from the frequency tuning curves of the natural resonator modes subject to a weak resonant drive, even for the signal parametric resonance (f_1) and the natural out-of-plane mode (f_{out}). We attribute this to the high amplitudes of the parametric resonances compared to the amplitudes of the two modes when linearly driven on resonance. The electric field gradient of the inhomogeneous electric field can only be linearized as a function of the dc voltage in the limit of small deflections of the string resonator [45], which gives rise to the quadratic tuning of f_{out} , whereas a modified tuning curve is expected for f_1 .

Additionally, we observe two satellite resonances, which are offset from the parametric resonances by their frequency difference and hence correspond to their beat note [42,43]. We interpret the appearance of the two satellites as the third-order nonlinear process of degenerate four-wave mixing [1] since the frequencies of the satellites can be expressed as mixing products of the present oscillation frequencies:

$$f_3 = 2f_1 - f_2, \quad f_4 = 2f_2 - f_1. \quad (2)$$

In Fig. 1(b) the calculated frequencies following Eq. (2) are displayed as blue daggers and they perfectly match the satellite frequencies extracted from the experimental data. Moreover, the frequency tuning of the satellites with applied dc voltage follows exactly the trend expected from Eq. (2). Note that the frequency sum of the satellite resonances always equals the pump frequency, $f_3 + f_4 = f_1 + f_2 = f_d = 2f_c$.

As the parametric resonances are tuned closer to each other, at a voltage of -14.31 V corresponding to a frequency difference of 2.41 kHz, the two modes suddenly lock to a single, extremely narrow high amplitude line and remain frequency locked for dc voltages exceeding the measurement span. The frequency of the line ($f_5 = 6.59082$ MHz) equals exactly half of the pump frequency,

$$f_5 = \frac{1}{2}f_d = f_c. \quad (3)$$

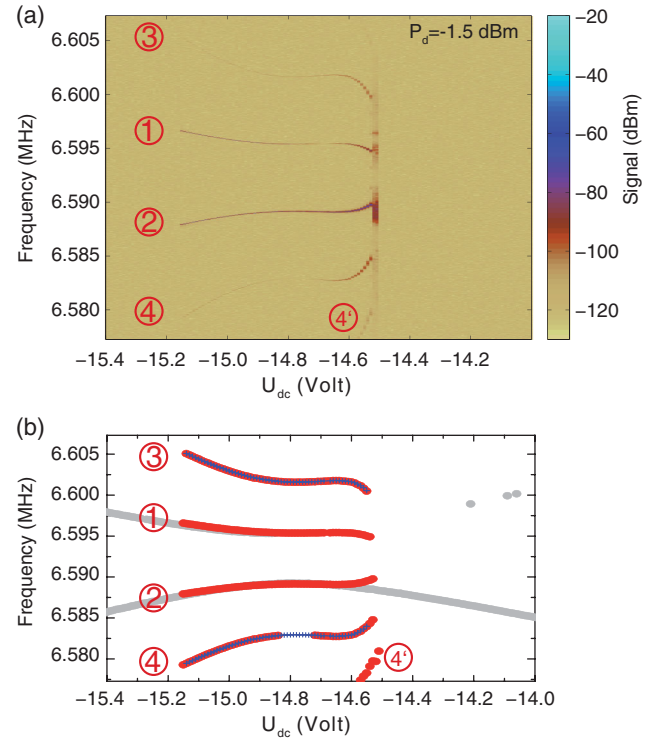


FIG. 2. (a) Color-coded frequency spectra versus dc voltage for a weak parametric drive power $P_d = -1.5$ dBm at $f_d = 13.18454$ MHz. Parametric oscillation resonances (f_1 , f_2), satellites from degenerate four-wave mixing (f_3 , f_4), a higher order satellite ($f_{4'}$), and a chaotic regime are observed. (b) The extracted peak frequencies of the above spectra (red dots) and calculated satellite resonances from Eq. (2) (blue daggers) exhibit excellent agreement. The gray dots display the avoided crossing of the two modes under a weak resonant drive with a mode splitting of 6.16 kHz. Some gray dots are missing for the in-plane mode due to the bad detection efficiency of this mode.

We attribute this threshold effect to the appearance of injection locking [3,4] of the two mechanical modes to half of the common pump frequency due to degenerate parametric two-mode oscillation (DP2O). As can be deduced from the extremely large locking range, this state is highly stable against perturbations of the system, in this case against the tuning of the natural resonance frequencies of the two modes. While the natural in-plane (f_{in}) and out-of plane (f_{out}) resonances are detuned by approximately 12.5 kHz at the end of the measurement span, corresponding to roughly 500 times their resonance linewidth, the injection locking still persists. Moreover, the two coupled flexural modes of the nanomechanical string resonator locked to the same frequency [26] can be considered as a mechanical analog of an electrical quadrature LC oscillator following the work of Mirzaei *et al.* [12].

Figures 2(a) and 2(b) depict the results of the same measurement scheme for a weak parametric drive of power $P_d = -1.5$ dBm and a different drive frequency $f_d = 13.18454$ MHz. Again, we observe NDP2O (f_1 , f_2) and D4WM (f_3 , f_4) starting at $U_{\text{dc}} = -15.15$ V. In

addition, another satellite ($f_{4'}$) appears at the bottom in Fig. 2. The additional satellite has the same spacing from f_4 as the first-order satellites (f_3, f_4) from the signal and idler resonance (f_1, f_2). The symmetric counterpart of this second-order satellite resonance is barely visible at the top of Fig. 2(a) with a too small signal power for the peak frequency extraction of the color-coded data. The appearance of second-order satellite resonances can again be interpreted as a D4WM process of the signal-idler frequencies and the first-order satellites ($f_{4'} = 2f_4 - f_2$). Equivalently expressed, the beat note between the signal and the idler creates satellite resonances that are offset by integer multiples of their beat note similar to those observed with conceptually different approaches [42,43].

Interestingly, the two parametric resonances do not exhibit injection locking to the pump in this experiment since the parametric drive is not strong enough to overcome the threshold of injection locking. Instead, the signal and idler enter a chaotic regime at $U_{dc} = -14.54$ V and disappear after a short dc voltage range [31,42,51].

Note that the coupling strength is 6.16 kHz in this measurement although the experiment is conducted on the same sample. Under continuous large-amplitude vibration, a decrease of the coupling strength was observed, which we attribute to a reduction of the electrical polarizability of the silicon nitride string as detailed in the Supplemental Material [44].

In Figs. 3(a) and 3(b) we show the results of the experiment for an intermediate parametric drive power $P_d = 13$ dBm at a drive frequency $f_d = 13.18502$ MHz, where the coupling of the modes is extracted as 1.87 kHz from the avoided crossing data. Analogous to the above measurements, the system exhibits signal and idler resonances via NDP2O and satellite resonances offset by their beat note starting at $U_{dc} = -14.65$ V. When the modes are tuned closer towards each other in frequency, they enter a chaotic regime similar to the results in Fig. 2. At a dc voltage of $U_{dc} = -14.20$ V, the modes start to lock to half of the drive frequency $f_5 = f_d/2$ out of the chaotic regime. However, the drive power is apparently not high enough to completely lock the two modes to the common drive. Interestingly, the system exhibits additional resonances compared to the strong pump experiment in Fig. 1. The satellite resonances (f_6 to f_{11}) are equidistantly offset from the locked resonance by integer multiples of a frequency f_b that increases with the dc voltage. Following the work of Razavi [11], we attribute the appearance of the satellites to the process of injection pulling [11] in combination with the observed partial injection locking to f_5 [6–9,24,26]. In the work of Razavi [11], the appearance of injection-pulled satellite resonances in a single quasi-locked electrical oscillator was found only on the positive frequency offset side of the injection locking peak at $f_{inj} + nf_b = f_d/2 + nf_b$ ($n=1,2,3,\dots$). The frequency offset from the injection locking frequency f_{inj} equals $f_b = [(f_0 - f_{inj})^2 - \delta^2]^{1/2}$, where

$$\delta \approx \frac{f_0 A_{inj}}{2Q A_0} \quad (4)$$

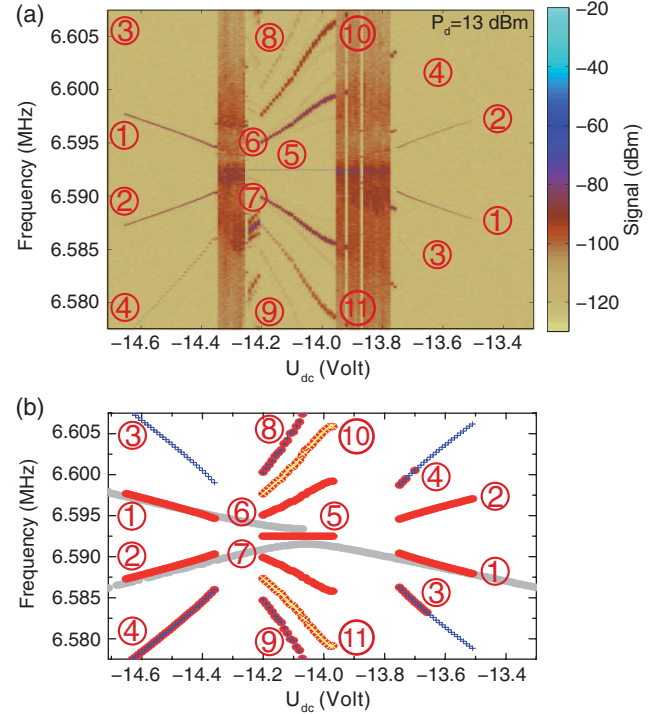


FIG. 3. (a) Color-coded frequency spectra versus dc voltage for an intermediate parametric drive power $P_d = 13$ dBm at $f_d = 13.18502$ MHz. Parametric oscillation resonances (f_1, f_2), satellites from degenerate four-wave mixing (f_3, f_4), and a partial injection locking peak (f_5) are observed. Additionally, equidistant injection pulling peaks appear (f_6 to f_{11}). (b) The extracted peak frequencies of the above spectra (red dots) and calculated satellite resonances from Eq. (2) (blue daggers, yellow crosses) exhibit excellent agreement. The gray dots display the avoided crossing of the two modes under a weak resonant drive with mode splitting of 1.87 kHz. Some gray dots are missing for the in-plane mode due to bad detection efficiency of this mode.

represents the maximum locking range, which depends on the amplitude ratio of the quasi-injection-locked oscillation (A_{inj}) and the oscillation (A_0) at the natural resonance frequency f_0 . In this work, the partial locking of two strongly coupled resonator modes to the common drive leads to additional injection-pulled satellites at $f_d/2 - nf_b$, the negative frequency offset side of the injection locking peak. The observed satellite resonances are completely axial symmetric with respect to the partial locking resonance.

Furthermore, assuming that f_5, f_6 , and f_7 are present, the remaining satellites can as well be obtained by frequency mixing,

$$\begin{aligned} f_8 &= 2f_6 - f_7, & f_9 &= 2f_7 - f_6, \\ f_{10} &= 2f_6 - f_5, & f_{11} &= 2f_7 - f_5, \end{aligned} \quad (5)$$

depicted as blue daggers and yellow crosses in Fig. 3(b).

By further detuning the natural resonance frequencies from the avoided crossing via the dc voltage, the partial locked and injection pulled state translates into another

chaotic regime. At a voltage of $U_{dc} = -13.75$ V the signal and idler resonances reappear out of the chaotic regime and resemble the dynamics of the system on the left-hand side of the avoided crossing until the parametric oscillation vanishes at $U_{dc} = -13.51$ V. A comparison of the data provided in Fig. 3 to the model of Adler [4] is carried out in the Supplemental Material [44].

In conclusion, we investigated the dynamics of two strongly coupled, high quality factor nanomechanical resonator modes subject to a common parametric drive in different parametric driving regimes. Depending on the driving strength and the frequency spacing of the two modes, we observed signal-idler generation via NDP2O in combination with satellite resonances at their beat-note frequency, partial injection locking, and two-mode injection pulling, as well as complete injection locking of the two coupled modes to the common drive frequency by DP2O. By individually tuning the frequency separation of the NDP2O, we demonstrated universal control of the nanomechanical signal-idler pair in all examined parametric driving regimes, which opens up the path towards parametric control in multimode nanoelectromechanics.

An integration of phase read-out technology into the presented experimental setup will allow for the implementation of passive phase noise cancellation approaches [52] over a large range of frequencies.

Moreover, the high mechanical quality factors in combination with the dielectric control of the system will allow for the study of correlated phase noise dynamics [53] without the need to add extra noise to the system.

Financial support by the Deutsche Forschungsgemeinschaft via the collaborative research center SFB 767 is gratefully acknowledged. M. A. acknowledges support by the Alexander von Humboldt Foundation via a fellowship for postdoctoral researchers. M. J. H. acknowledges support by the Deutsche Forschungsgemeinschaft via the Emmy Noether fellowship HA 5593/1-1. Furthermore, we thank Andreas Isacsson, Yaroslav Blanter, and Gianluca Rastelli for fruitful discussions. Preliminary experiments on the topic performed by Onur Basarir and Johannes Rieger are gratefully acknowledged.

*maximilian.seitner@uni-konstanz.de

- [1] B. E. A. Saleh and M. C. Teich, *Fundamentals of Photonics*, 2nd ed. (Wiley-Interscience, New York, 2007).
- [2] A. Yariv, *Quantum Electronics*, 2nd ed. (John Wiley & Sons, New York, 1975), pp. 437ff.
- [3] C. J. Buczek, R. J. Freiberg, and M. L. Skolnick, *Proc. IEEE* **61**, 1411 (1973).
- [4] R. Adler, *Proc. IEEE* **61**, 1380 (1973).
- [5] V. Annovazzi-Lodi, S. Donati, and M. Manna, *IEEE J. Quantum Electron.* **30**, 1537 (1994).
- [6] V. Annovazzi-Lodi, A. Scire, M. Sorel, and S. Donati, *IEEE J. Quantum Electron.* **34**, 2350 (1998).
- [7] G. Liu, X. Jin, and S. L. Chuang, *IEEE Photonics Technol. Lett.* **13**, 430 (2001).
- [8] Y. Liu, P. Davis, Y. Takiguchi, T. Aida, S. Saito, and J.-M. Liu, *IEEE J. Quantum Electron.* **39**, 269 (2003).
- [9] H. L. Stover, *Proc. IEEE* **54**, 310 (1966).
- [10] K. Chang, K. A. Hummer, and J. L. Klein, *IEEE Trans. Microwave Theory Tech.* **37**, 1078 (1989).
- [11] B. Razavi, *IEEE J. Solid-State Circuits* **39**, 1415 (2004).
- [12] A. Mirzaei, M. E. Heidari, R. Bagheri, S. Chehrizi, and A. A. Abidi, *IEEE J. Solid-State Circuits* **42**, 1916 (2007).
- [13] M. Abel, *J. Acoust. Soc. Am.* **119**, 2467 (2006).
- [14] M. Abel, K. Ahnert, and S. Bergweiler, *Phys. Rev. Lett.* **103**, 114301 (2009).
- [15] Y.-Y. Liu, J. Stehlik, M. J. Gullans, J. M. Taylor, and J. R. Petta, *Phys. Rev. A* **92**, 053802 (2015).
- [16] D. Rugar and P. Grütter, *Phys. Rev. Lett.* **67**, 699 (1991).
- [17] K. L. Turner, S. A. Miller, P. G. Hartwell, N. C. MacDonald, S. H. Strogatz, and S. G. Adams, *Nature (London)* **396**, 149 (1998).
- [18] J. P. Mathew, R. N. Patel, A. Borah, R. Vijay, and M. M. Deshmukh, *Nat. Nanotechnol.* **11**, 747 (2016).
- [19] A. Leuch, L. Papariello, O. Zilberberg, C. L. Degen, R. Chitra, and A. Eichler, *Phys. Rev. Lett.* **117**, 214101 (2016).
- [20] I. Mahboob, H. Okamoto, K. Onomitsu, and H. Yamaguchi, *Phys. Rev. Lett.* **113**, 167203 (2014).
- [21] Y. S. Patil, S. Chakram, L. Chang, and M. Vengalattore, *Phys. Rev. Lett.* **115**, 017202 (2015).
- [22] A. Pontin, M. Bonaldi, A. Borrielli, L. Marconi, F. Marino, G. Pandraud, G. A. Prodi, P. M. Sarro, E. Serra, and F. Marin, *Phys. Rev. Lett.* **116**, 103601 (2016).
- [23] I. Mahboob, H. Okamoto, and H. Yamaguchi, *New J. Phys.* **18**, 083009 (2016).
- [24] M. C. Cross, A. Zumdieck, R. Lifshitz, and J. L. Rogers, *Phys. Rev. Lett.* **93**, 224101 (2004).
- [25] G. Heinrich, M. Ludwig, J. Qian, B. Kubala, and F. Marquardt, *Phys. Rev. Lett.* **107**, 043603 (2011).
- [26] J. Thévenin, M. Romanelli, M. Vallet, M. Brunel, and T. Erneux, *Phys. Rev. Lett.* **107**, 104101 (2011).
- [27] C. A. Holmes, C. P. Meaney, and G. J. Milburn, *Phys. Rev. E* **85**, 066203 (2012).
- [28] P. Del'Haye, K. Beha, S. B. Papp, and S. A. Diddams, *Phys. Rev. Lett.* **112**, 043905 (2014).
- [29] T. Barois, S. Perisanu, P. Vincent, S. T. Purcell, and A. Ayari, *New J. Phys.* **16**, 083009 (2014).
- [30] T. Li, T.-Y. Bao, Y.-L. Zhang, C.-L. Zou, X.-B. Zou, and G.-C. Guo, *Opt. Express* **24**, 12336 (2016).
- [31] M. Bagheri, M. Poot, L. Fan, F. Marquardt, and H. X. Tang, *Phys. Rev. Lett.* **111**, 213902 (2013).
- [32] D. K. Agrawal, J. Woodhouse, and A. A. Seshia, *Phys. Rev. Lett.* **111**, 084101 (2013).
- [33] M. H. Matheny, M. Grau, L. G. Villanueva, R. B. Karabalin, M. C. Cross, and M. L. Roukes, *Phys. Rev. Lett.* **112**, 014101 (2014).
- [34] J. Gieseler, M. Spasenović, L. Novotny, and R. Quidant, *Phys. Rev. Lett.* **112**, 103603 (2014).
- [35] S. Y. Shah, M. Zhang, R. Rand, and M. Lipson, *Phys. Rev. Lett.* **114**, 113602 (2015).
- [36] M. Zhang, S. Shah, J. Cardenas, and M. Lipson, *Phys. Rev. Lett.* **115**, 163902 (2015).

- [37] S.-B. Shim, M. Imboden, and P. Mohanty, *Science* **316**, 95 (2007).
- [38] M. Hossein-Zadeh and K.J. Vahala, *Appl. Phys. Lett.* **93**, 191115 (2008).
- [39] C. Huang, J. Fan, R. Zhang, and L. Zhu, *Appl. Phys. Lett.* **101**, 231112 (2012).
- [40] M. Zhang, G. S. Wiederhecker, S. Manipatruni, A. Barnard, P. McEuen, and M. Lipson, *Phys. Rev. Lett.* **109**, 233906 (2012).
- [41] D. Antonio, D. A. Czaplowski, J. R. Guest, D. López, S. I. Arroyo, and D. H. Zanette, *Phys. Rev. Lett.* **114**, 034103 (2015).
- [42] E. Gil-Santos, M. Labousse, C. Baker, A. Goetschy, W. Hease, C. Gomez, A. Lemaître, G. Leo, C. Ciuti, and I. Favero, *Phys. Rev. Lett.* **118**, 063605 (2017).
- [43] A. Ganesan, C. Do, and A. Seshia, *Phys. Rev. Lett.* **118**, 033903 (2017).
- [44] See Supplemental Material at <http://link.aps.org/supplemental/10.1103/PhysRevLett.118.254301> for the experimental setup, the influence of the drive power on the coupling strength and the comparison of the experimental results to the Adler equation.
- [45] J. Rieger, T. Faust, M. J. Seitner, J. P. Kotthaus, and E. M. Weig, *Appl. Phys. Lett.* **101**, 103110 (2012).
- [46] T. Faust, J. Rieger, M. J. Seitner, P. Krenn, J. P. Kotthaus, and E. M. Weig, *Phys. Rev. Lett.* **109**, 037205 (2012).
- [47] T. Faust, J. Rieger, M. J. Seitner, J. P. Kotthaus, and E. M. Weig, *Nat. Phys.* **9**, 485 (2013).
- [48] M. J. Seitner, H. Ribeiro, J. Kölbl, T. Faust, J. P. Kotthaus, and E. M. Weig, *Phys. Rev. B* **94**, 245406 (2016).
- [49] T. Faust, P. Krenn, S. Manus, J. P. Kotthaus, and E. M. Weig, *Nat. Commun.* **3**, 728 (2012).
- [50] A. Olkhovets, D. Carr, J. Parpia, and H. Craighead, in *The 14th IEEE International Conference on Micro Electro Mechanical Systems*, Micro Electro Mechanical Systems (IEEE, New York, 2001), p. 298.
- [51] R. B. Karabalin, M. C. Cross, and M. L. Roukes, *Phys. Rev. B* **79**, 165309 (2009).
- [52] E. Kenig, M. C. Cross, R. Lifshitz, R. B. Karabalin, L. G. Villanueva, M. H. Matheny, and M. L. Roukes, *Phys. Rev. Lett.* **108**, 264102 (2012).
- [53] F. Sun, X. Dong, J. Zou, M. I. Dykman, and H. Chan, *Nat. Commun.* **7**, 12694 (2016).